

Simulation and finite element analysis of continuous multi-pass hot rolled AZ31B magnesium alloy sheets

K. Yu*, Z. Y. Cai, X. Tan, F. W. Chen, Y. N. Hu, S. J. Li

School of Materials Science and Engineering, Central South University, Changsha 410083, China

Received 27 September 2010, received in revised form 8 February 2011, accepted 8 February 2011

Abstract

The deformation behavior of the continuous multi-pass hot rolling AZ31B sheets is tested in a Gleeble 1500 thermo-mechanical simulator. The evolution of microstructure during the deformation process is observed and the constitutive relation of AZ31B alloy is analyzed by a finite element method. The results show that the deformation behavior of continuous multi-pass hot rolling of AZ31B sheets is totally different with that of single pass rolling. The work hardening mechanism plays a more important role than the dynamic recrystallization does during the continuous multi-pass deformation process under different strain rates from 0.01 s^{-1} to 5 s^{-1} . The calculated value of high temperature deformation activation energy of hot rolling AZ31B sheets is 171 kJ mol^{-1} . The FEM simulation provides a detailed distribution of temperatures, stress and equivalent strains in the continuous multi-pass rolling sheet.

Key words: magnesium alloys, finite element analysis, rolling, thermo-mechanical processing

1. Introduction

Magnesium (Mg) alloys offer light weight, high stiffness, excellent machinability and superior damping capacity. It has a great potential to be used in different metal parts to reduce the weight [1]. The Mg alloys possess limited ductility, mostly because of their hexagonal closed-packed (HCP) lattice [2, 3]. Plastic deformation of AZ31B Mg alloy has been investigated because such alloy is suited for wrought products such as the sheets produced by rolling [4]. A lot of experimental researches [5–7] have been made to investigate the properties, microstructure and plastic deformation behavior of wrought AZ31B alloy sheet. But as is well understood, the AZ31B alloy sheets will endure continuous multi-pass rolling between annealing treatment during the hot rolling process in the industry conditions. During the continuous multi-pass rolling passes, the deformation parameters such as the sheet temperatures, the deformation strain rates and the deformation degrees will change greatly. All of these variations will lead to a total different deformation behavior compared with a single pass rolling AZ31B sheets. In this investigation, the continuous multi-pass

hot rolling of AZ31B alloy sheets are performed by using an experimental simulation and a finite element analysis (FEA). All the parameters used in the investigations are based on the industrial deformation processing, and the parameters of rolling mill machine are actually used in CHINALCO Luoyang Copper Co. Ltd. The results provide data for comprehending the continuous multi-pass hot rolling behavior and optimize the hot rolling process of AZ31B magnesium alloy sheet.

2. Experimental methods

The direct chilled casting AZ31B alloy billets used in the present study were provided by CHINALCO Luoyang Copper Co. Ltd. The chemical composition of this alloy was Mg-2.74%Al-0.97%Zn-0.33%Mn. The cylindrical specimens with a diameter of 10 mm and a height of 15 mm were machined from the billets for the experimental simulation [8]. A uniaxial hot compression tests were performed on Gleeble 1500 thermo-mechanical simulator under different strain rates of 0.01 s^{-1} , 0.1 s^{-1} , 1 s^{-1} , and 5 s^{-1} . The strain rates

*Corresponding author: tel.: +86-731-88879341; fax: +86-731-88876692; e-mail address: yukun@csu.edu.cn

Table 1. Parameters of AZ31B alloy during the deformation experiment simulation

Rolling pass	Temperature (°C)	Thickness before deformation (mm)	Thickness after deformation (mm)	Deformed degree (%)
1	500	15	13.37	10.9
2	490	13.37	11.65	12.9
3	480	11.65	10.01	14.1
4	470	10.01	8.37	16.4
5	460	8.37	6.82	18.5
6	450	6.82	5.46	20
7	440	5.46	4.28	21.7
8	430	4.28	3.37	21.3
9	420	3.37	2.64	21.6
10	400	2.64	2.18	17.24
11	380	2.18	1.82	16.7

Table 2. The parameters of AZ31B alloy applied in the FEA simulation

Temperature (°C)	125	175	225	275	325	375	425	475
Young's modulus (GPa)	41.86	40.93	40.00	39.53	38.37	36.98	36.51	35.35
Temperature (°C)	100	150	200	250	300	400		
Thermal conductivity (W m ⁻¹ K ⁻¹)	87.3	92.4	97.0	101.8	106.0	114.0		
Temperature (°C)	20–100	100	200	300	400			
Specific heat (kJ kg ⁻¹ K ⁻¹)	1.05	1.13	1.17	1.21	1.26			

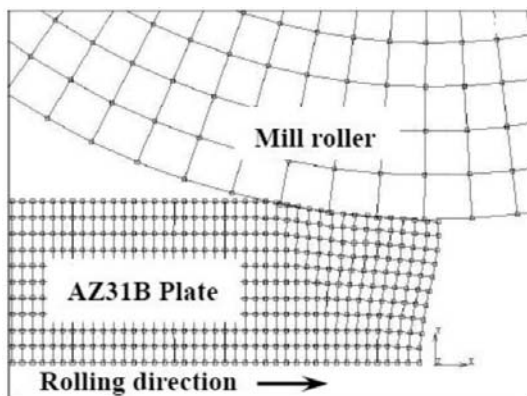


Fig. 1. FEA model of continuous multi-pass hot rolling AZ31B alloy sheet.

represented the rolling speeds that the mill could perform actually in the industry. The detail parameters performed in the test are shown in Table 1.

The simulation was performed by using elastic-plastic finite element methods (FEM) with the commercial software MSC/MARC. The FEA model which was employed in this study is illustrated in Fig. 1. The input parameters of AZ31B alloy in the finite element simulation are listed in Table 2 [4]. The density of AZ31B alloy is $1.78 \times 10^3 \text{ kg m}^{-3}$, and the Poisson's ratio is 0.3. The density of mill roller is

$7.85 \times 10^3 \text{ kg m}^{-3}$, the elastic modulus is 210 GPa, and the Poisson's ratio is 0.33 [9]. For the sake of simplicity, the rollers were considered to be rigid bodies but the AZ31 alloy sheets were regarded as two-dimensional deformable bodies. Microstructures of the specimens were examined by the Tecnai G² 20 transmission electron microscope (TEM).

3. Results and discussion

3.1. Experimental simulation of continuous multi-pass hot rolling of AZ31B alloy sheet

The true stress-strain curves of continuous multi-pass hot deforming AZ31B alloy under different strain rates and with different temperatures are shown in Fig. 2a–d. The decreasing of temperatures (as shown in Table 1) represents the variation of temperatures during the continuous rolling process. The curves show that the strain rate has a great effect on the deformed stress of AZ31B alloy. With a relative low strain rate of 0.01 s^{-1} , the stable stress value is about 40 MPa. But it increases obviously with the increasing of strain rate. The value of stable stress obtains about 80 MPa with a strain rate of 5 s^{-1} which is a normal rolling speed applied in the industry to ensure the manufacture efficiency. The true stress-strain curves of continuous multi-pass rolling show a totally different be-

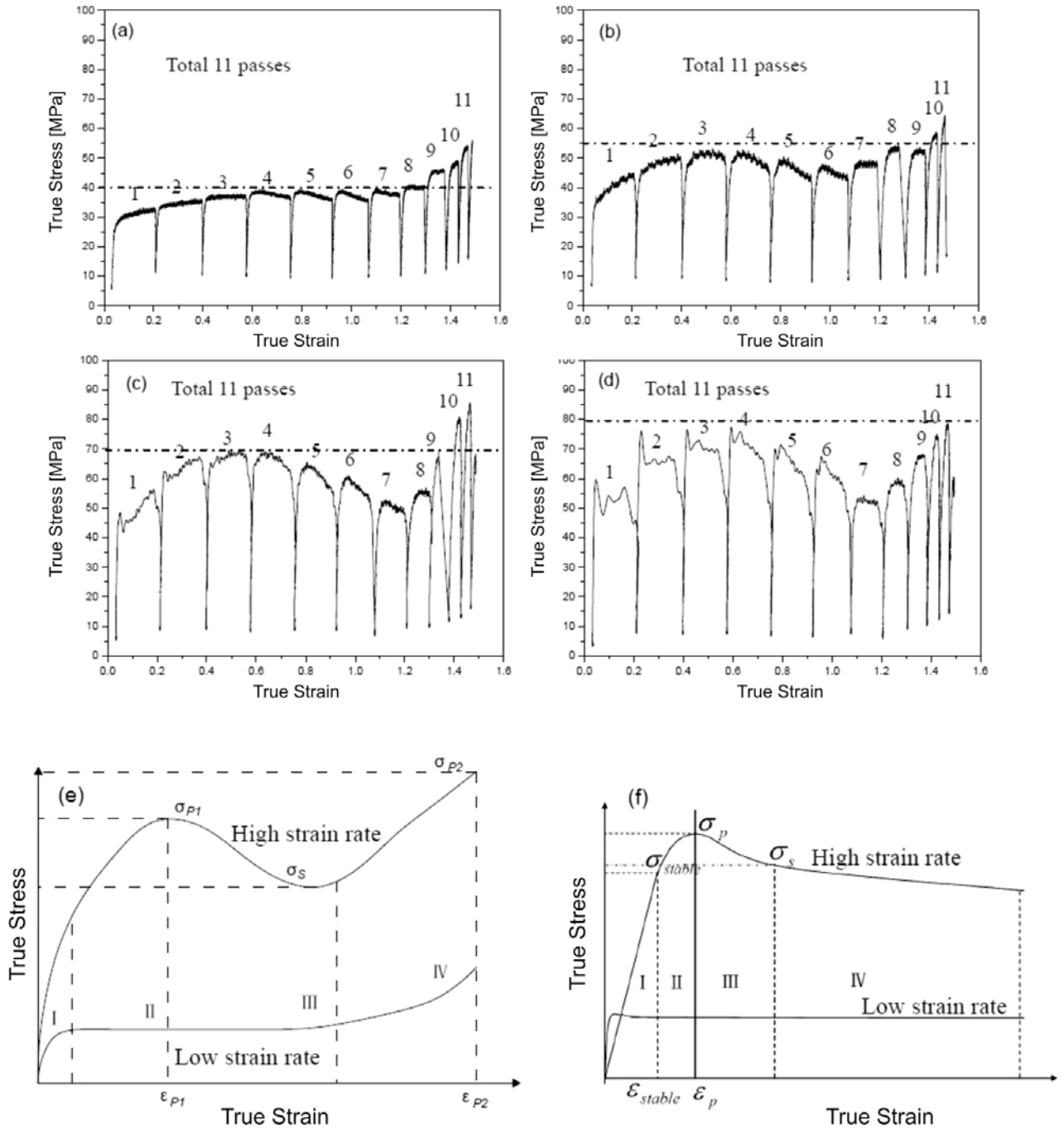


Fig. 2. True stress-strain curves of continuous multi-pass hot rolling AZ31B alloy: (a) strain rate of 0.01 s^{-1} , (b) strain rate of 0.1 s^{-1} , (c) strain rate of 1 s^{-1} , (d) strain rate of 5 s^{-1} , (e) schematic curves of multi-pass hot rolling AZ31B alloy, (f) schematic curves of single pass hot rolling AZ31B alloy [4].

havior with single deformed true stress-strain curves as shown in Fig. 2e,f. Figure 2e shows schematic curves of continuous multi-pass rolling of AZ31B sheet. On a low strain rate condition (such as 0.01 s^{-1} in Fig. 2a), the curve shows a stable stress during the whole deformed process. It is similar to the curve of AZ31 alloy with a low strain rate under the single pass deformation as shown in Fig. 2f. But the difference is that the stress increases in the end of multi-pass rolling due to

the work hardening effect. On a high strain rate condition (such as 5 s^{-1} in Fig. 2d), the continuous multi-pass rolling stress curve shows two peak values during the deformed process. One is in the beginning stage of deformation (as shown in passes 3 and 4 in Fig. 2d). The other is in the end of the deformation process (as shown in passes 9–11 in Fig. 2d). It can be anticipated that the work hardening mechanism dominated the deformed behavior during the whole deformation

process [10]. The stress will decrease only from pass 5 to pass 7 due to a temporary dynamic recrystallization (DRX) softening.

The schematic curves show a different deformation behavior of AZ31B alloy between the multi-pass and the single pass deformed process because different mechanisms influence the deforming process. Work hardening and DRX softening are treated as two main mechanisms that influence the deforming behavior of AZ31B sheets [11, 12]. During the continuous multi-pass hot deformation, the work hardening mechanism plays an obviously more important role during the passes than the DRX does even on a high temperature over 380°C. Although the DRX softening is the main mechanism that dominates the behavior of AZ31B alloy in a single deforming process [13], the work hardening mechanism influences the plastic deformation behaviors obviously both at the beginning and the ending stage of the alloy in multi-pass deformation. The microstructure evolutions also show that both the dislocations and twins are appeared obviously at the beginning of deformation after pass 3 (Fig. 3a). Some DRX grains surrounded with dislocations appear during pass 5 to pass 7 (Fig. 3b). This is the reason that the stress value decreases a little during that period. Soon a lot of dislocations and twins appear in the alloy after pass 9 (Fig. 3c) so that the stress values increase with such work hardening effect. The evolution of stress-strain curves is accompanied with the variation of microstructures.

3.2. Constitutive relation of hot rolling AZ31B alloy sheet

From the stress-strain curves of AZ31B alloy samples, the constitutive relation of AZ31B alloy during the deformation can be calculated. It is evident that the temperatures and strain rates have great effects on the flow stress and the deformation properties of AZ31B alloy [14]. A function of the strain rate can be used to describe the plastic deforming character of AZ31B alloy. It can be given in terms of the stress σ , temperature T , state variables S_i and material constant P_i (it remains constant for a given material such as AZ31B alloy) from Eq. (1) [15]:

$$\dot{\epsilon} = f(\sigma, T, S_i, P_i). \quad (1)$$

In this equation, the stress is an independent variable. Investigations of different hot working data demonstrate that the mathematic relationship between σ and $\dot{\epsilon}$ can be described as follows [15]:

$$\dot{\epsilon} = A[\sinh(\alpha\sigma)]^n \exp\left(-\frac{Q}{RT}\right), \quad (2)$$

where A and α ($= 0.0178 \text{ MPa}^{-1}$ for Mg alloy) are

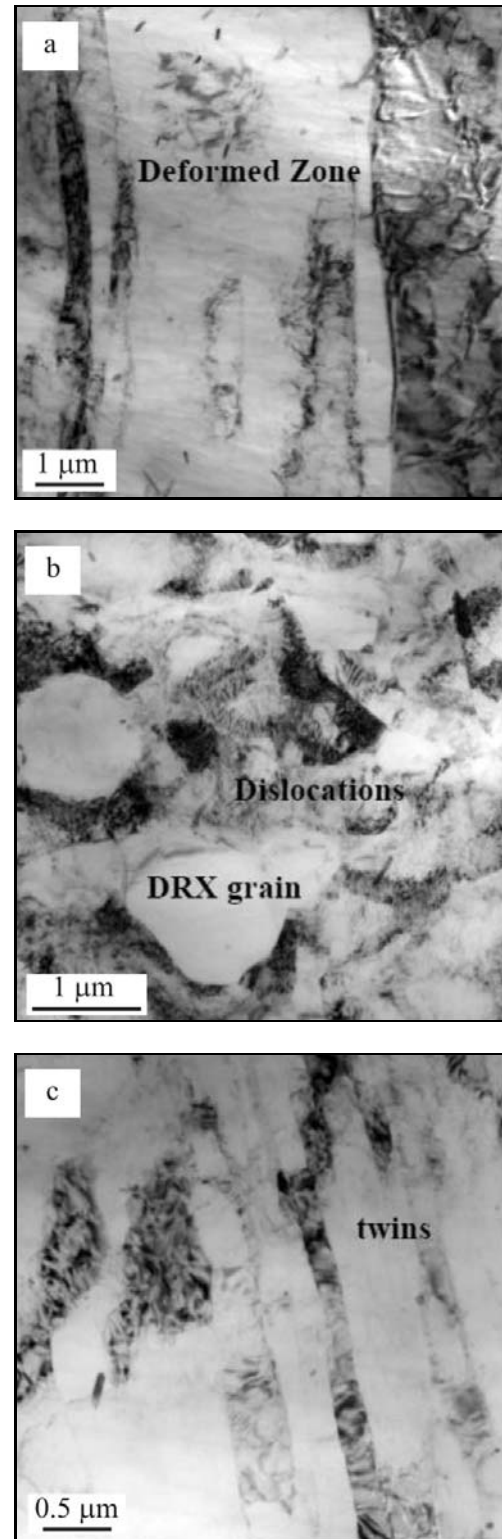


Fig. 3. Images showing the TEM morphology of AZ31B alloy on different hot deformation passes: (a) microstructure after pass 3, (b) microstructure after pass 6, (c) microstructure after pass 9.

material constants, n is the stress exponent, R is the gas constant ($= 8.314 \text{ J mol}^{-1} \text{ K}^{-1}$), T is the deforma-

ation temperature (K), and Q is the activation energy (kJ mol^{-1}) for high-temperature deformation. This relationship also includes the dynamic equilibrium with work hardening and DRX softening during hot working.

Constitutive equations are commonly used to calculate the flow stresses of a material deformation. The Arrhenius equation is widely used to describe the relationship between the deformation temperature, strain rate and flow stress, especially at elevated temperature. In the kinetic analysis, it is customary to correlate the temperature and strain rate dependence of flow stress with Zener-Hollomon parameter Z [15]. For the present constitutive analysis of the hot deformation behavior of AZ31B alloy, the following sine hyperbolic equation is used:

$$A[\sinh(\alpha\sigma)]^n = \dot{\epsilon} \exp\left(\frac{Q}{RT}\right) = Z. \quad (3)$$

Z is the Zener-Hollomon parameter connecting the two control variables through an Arrhenius equation with apparent activation energy Q . The activation energy can be expressed as follows [15]:

$$Q = R \left\{ \frac{\partial \ln[\sinh(\alpha\sigma)]}{\partial(1/T)} \right\}_{\dot{\epsilon}} \left\{ \frac{\partial \ln \dot{\epsilon}}{\partial \ln[\sinh(\alpha\sigma)]} \right\}_T. \quad (4)$$

The value of high temperature deformation activation energy is calculated with a result of 171 kJ mol^{-1} . Though this value of the activation energy is quite close to the activation energy for self-diffusion in Mg (135 kJ mol^{-1}) or for diffusion of Al atoms in Mg (143 kJ mol^{-1}) [16], it is different from them because it reflects the nature of the mechanisms that both the work hardening and DRX influence the deforming behavior of AZ31B alloy. The calculated constitutive equation of AZ31B during the continuous multi-pass hot deformation is as follows:

$$\sigma = \frac{1}{0.022782} \ln \left\{ \left(\frac{z}{5.55 \times 10^{12}} \right)^{\frac{1}{5.8033}} + \left[\left(\frac{z}{5.55 \times 10^{12}} \right)^{\frac{2}{5.8033}} + 1 \right]^{\frac{1}{2}} \right\}, \quad (5)$$

where $Z = \dot{\epsilon} \exp\left(\frac{171 \times 10^3}{RT}\right)$.

3.3. Finite element analysis of continuous multi-pass hot rolling of AZ31B alloy

The distributions of temperature, stress and equivalent strain are simulated by using FEM as shown in

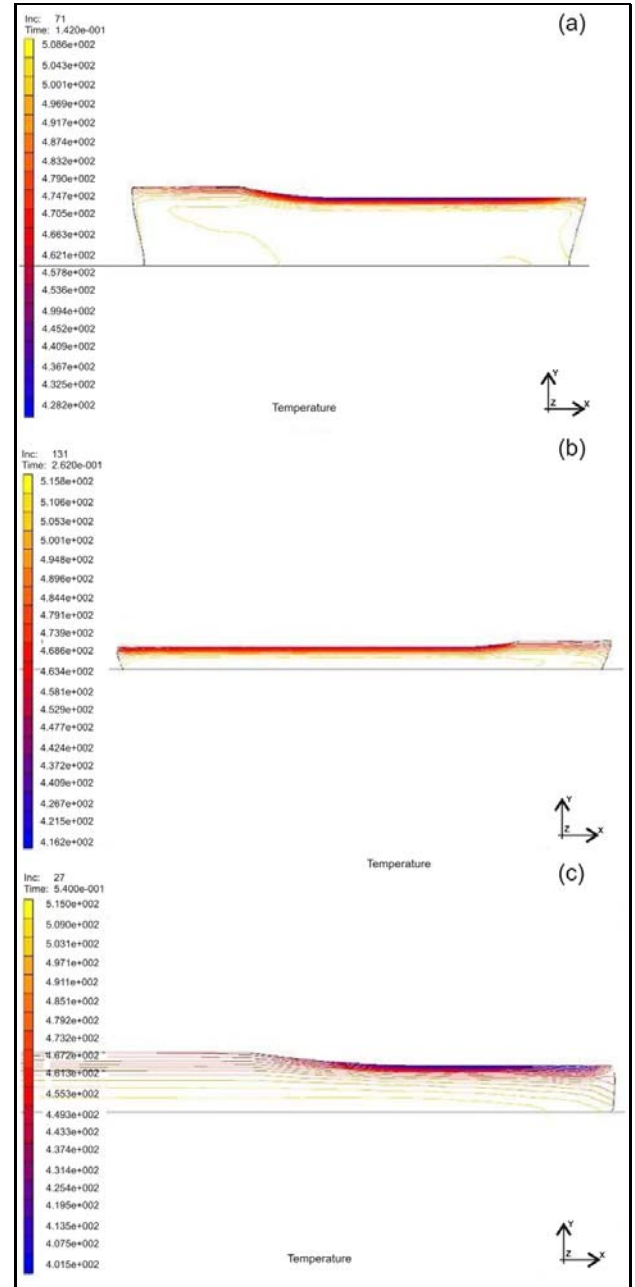


Fig. 4a,b,c. FEA simulation of AZ31B alloy during the hot rolling: (a) temperature distribution after pass 3, (b) temperature distribution after pass 6, (c) temperature distribution after pass 9.

Fig. 4. The typical simulation results after the pass 3, pass 6 and pass 9 are selected to be compared with the results of experimental deformation behavior and microstructure. The simulation shows that the temperatures in the inner parts of AZ31B alloy sheet are higher than those on the surface of sheet. So, the high temperature during the hot rolling leads to the DRX, especially during the rolling process from pass 5 to pass 7 because the deformed degree accumulates and

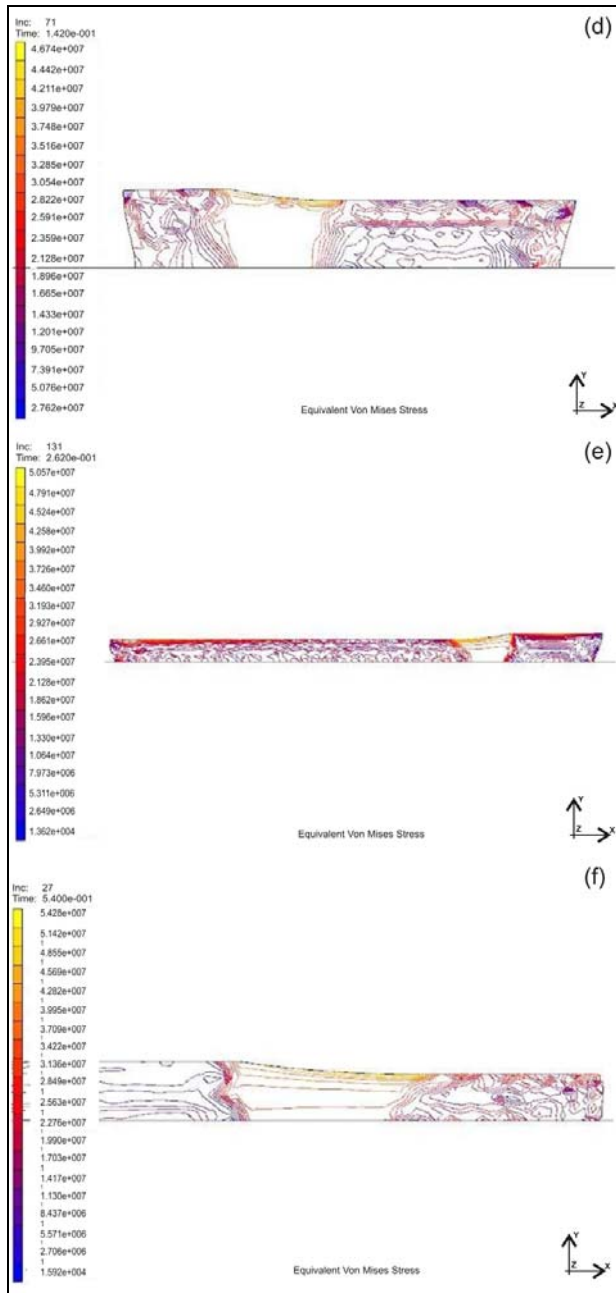


Fig. 4d,e,f. FEA simulation of AZ31B alloy during the hot rolling: (d) stress distribution after pass 3, (e) stress distribution after pass 6, (f) stress distribution after pass 9.

produces more deformed heat energy in the alloy. But the heat is transferred to the mill roller on the surface of the sheet, so that the temperature on the surface of sheet decreases. This leads to an obvious work hardening effect on the sheets. During a continuous rolling process, the heat diffusion through the mill roller is very high and the rolling process of AZ31B alloy is influenced. It is shown in Fig. 4 that the maximum value of tensile stress is distributed in the middle parts of the sheet. But since it is well known that the highest

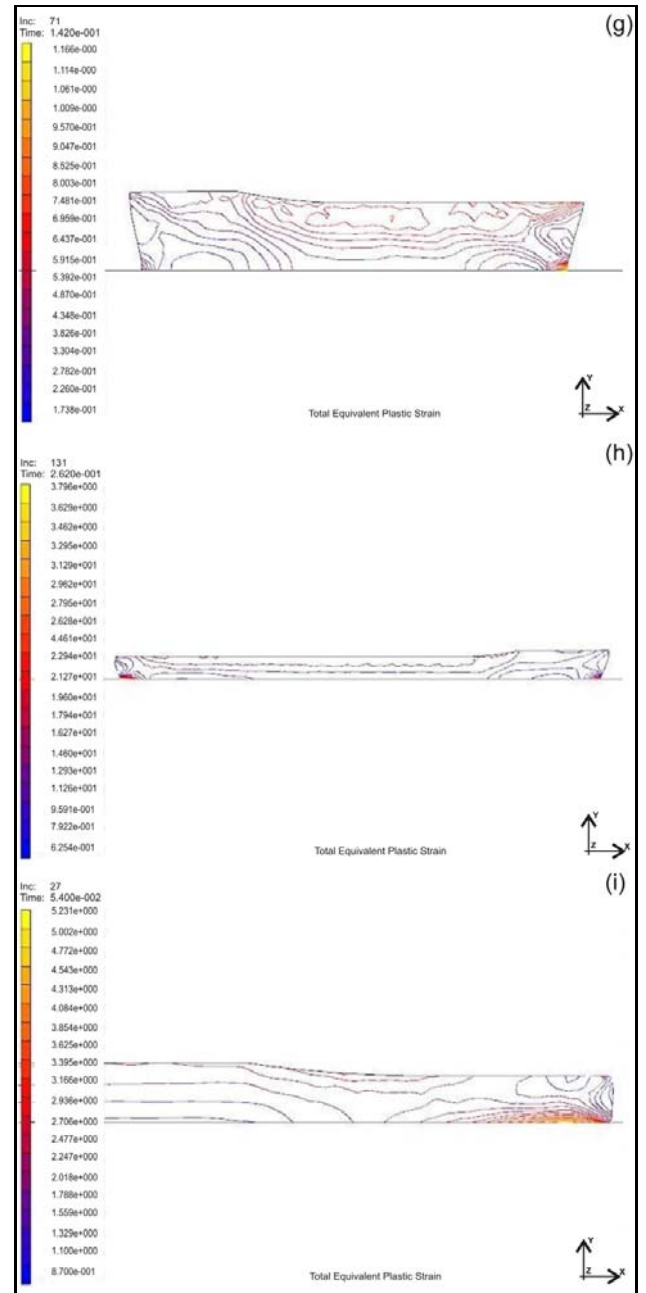


Fig. 4g,h,i. FEA simulation of AZ31B alloy during the hot rolling: (g) equivalent strain distribution after pass 3, (h) equivalent strain distribution after pass 6, (i) equivalent strain distribution after pass 9.

temperature is also in such a place, the sheet will not break during the rolling process if the temperature is high enough to meet the deformation requirements of AZ31B alloy sheet. Therefore, controlling the hot rolling temperature is so important as it influences the continuity of hot rolling process. It can be anticipated that if the temperature decreases, the AZ31B alloy sheets will break during the rolling process. The simulation shows that the strain distributes heterogeneous along the thickness of the sheet because the deform-

ation is heterogeneous along the thickness direction of sheet. This will lead to a different morphology of microstructure that the DRX grains or dislocations exist as shown in Fig. 3b. It can be deduced that the FEA simulation is in accordance with the rolling test and provides clear understanding of plastic deformation behavior of AZ31B alloy during the continuous multi-pass hot rolling.

4. Conclusions

1. The deformation behavior of continuous multi-pass hot rolling of AZ31B sheets is different from that of the single pass hot rolling. The work hardening mechanism plays an important role during the deformation process. The DRX that dominates in the single hot rolling process of AZ31B alloy is not as impact as in the multi-pass deformation process.

2. The high temperature deformation activation energy of deforming sheets is calculated with a result of 171 kJ mol^{-1} . The constitutive equation of AZ31B during the continuous multi-pass hot deformation can be obtained through the analysis and calculation of the data from the deformation tests performed on Gleeble 1500 thermo-mechanical simulator.

3. The FEA simulation provides a detailed distribution of temperature, stress and equivalent strain in the rolling sheet and it is useful to understand the deformed characteristic of AZ31B sheet during a continuous multi-pass hot rolling process.

Acknowledgements

Financial supports from A Canada-China-USA Collaborative Research & Development Project, Magnesium Front End Research and Development (MFERD) are gratefully acknowledged.

The authors acknowledge Dr H. F. Lou and Mr H. T. Liu from CHINALCO Luoyang Copper Co. Ltd for their technical assistance in providing the rolling mill machine parameters and AZ31B alloy ingots.

References

- [1] MORDIKE, B. L.—EBERT, T.: *Mater. Sci. Eng. A*, 302, 2001, p. 37. [doi:10.1016/S0921-5093\(00\)01351-4](https://doi.org/10.1016/S0921-5093(00)01351-4)
- [2] DECKER, R. F.: *Advanced Mater. and Proc.*, 154, 1998, p. 31.
- [3] KUBOTA, K.—MABUCHI, M.—HIGASHI, K.: *J. Mater. Sci.*, 34, 1999, p. 2255. [doi:10.1023/A:1004561205627](https://doi.org/10.1023/A:1004561205627)
- [4] AVEDESIAN, M. M.—BAKER, H.: *Magnesium and Magnesium Alloys*. Materials Park, Ohio, ASM International 1999.
- [5] SPIGARELLI, S.—MEHTEDI, M. E.—CABIBBO, M.—EVANGELISTA, E.—KANeko, J.—JÄGER, A.—GARTNEROVA, V.: *Mater. Sci. and Eng. A*, 462, 2007, p. 197.
- [6] YIN, D. L.—ZHANG, K. F.—WANG, G. F.—HAN, W. B.: *Mater. Sci. and Eng. A*, 392, 2005, p. 320.
- [7] PRASAD, Y. V. R. K.—RAO, K. P.: *Mater. Sci. and Eng. A*, 432, 2006, p. 170.
- [8] CERRI, E.—LEO, P.—MARCO, P. P. D.: *J. of Mater. Proc. Tech.*, 189, 2007, p. 97.
- [9] ARITZUR, B.: *Handbook of Metal-Forming Processes*. New York, John Wiley and Sons 2008.
- [10] YI, S. B.—DAVIES, C. H. J.—BROKMEIER, H. G.—BOLMARO, R. E.—KAINER, K. U.—HOMEYER, J.: *Acta Materialia*, 54, 2006, p. 549. [doi:10.1016/j.actamat.2005.09.024](https://doi.org/10.1016/j.actamat.2005.09.024)
- [11] MYSHLYAEV, M. M.—McQUEEN, H. J.—MWEMBELA, A.—KONOPLEVA, E.: *Mater. Sci. and Eng. A*, 337, 2002, p. 121. [doi:10.1016/S0921-5093\(02\)00007-2](https://doi.org/10.1016/S0921-5093(02)00007-2)
- [12] SAMMAN, T. A.—GOTTSTEIN, G.: *Mater. Sci. and Eng. A*, 490, 2008, p. 411.
- [13] McQUEEN, H. J.: *Mater. Sci. and Eng. A*, 387–389, 2004, p. 203. [doi:10.1016/j.msea.2004.01.064](https://doi.org/10.1016/j.msea.2004.01.064)
- [14] TAN, J. C.—TAN, M. J.: *Mater. Sci. and Eng. A*, 339, 2003, p. 124. [doi:10.1016/S0921-5093\(02\)00096-5](https://doi.org/10.1016/S0921-5093(02)00096-5)
- [15] McQUEEN, H. J.—RYAN, N. D.: *Mater. Sci. and Eng. A*, 322, 2002, p. 43. [doi:10.1016/S0921-5093\(01\)01117-0](https://doi.org/10.1016/S0921-5093(01)01117-0)
- [16] SLOOFF, F. A.—ZHOU, J.—DUSZCZYK, J.—KATGERMAN, L.: *Scripta Materialia*, 57, 2007, p. 759. [doi:10.1016/j.scriptamat.2007.06.023](https://doi.org/10.1016/j.scriptamat.2007.06.023)